JOURNAL OF MATERIALS SCIENCE 29 (1994) 1341–1347

Pulse chemical vapour deposition and infiltration of pyrocarbon in model pores with rectangular cross-sections

Part I *Study of the pulsed process of deposition*

P. DUPEL, R. PAILLER, F. LANGLAIS
Laboratoire des Composites Thermostructuraux UMR-47 CNRS-SEP-UB1, Domaine Universitaire 3 allée de La Boëtie, 33600 Pessac, France

Pulse chemical vapour deposition and infiltration is a promising technique for densifying porous substrates. By cycling the reactor pressure, the in-depth depletion of the gas phase is limited. An experimental approach of the deposition process is presented: for determining the influence of the residence time, temperature, pressure and nature of the precursor on the gas phase composition and the deposition thicknesses at the external surface and within the pores of the substrate. Two types of mechanism are involved, governed by the maturation of the gas phase during the pulse. For low pressures, low temperatures and stable precursors such as CH_4, the gas maturation is very limited, the deposition mainly occurs by slow decomposition of small molecules and good infiltration can be obtained. Conversely, for high pressures, high temperatures and more reactive precursors such as C_3H_8, a high maturation of the gas phase results in (i) rapid condensation of stacks of small carbon layers through heavy aromatic species and (ii) difficult infiltration of porous substrates.

1. Introduction

The ceramic matrix composites (CMC), developed mainly for aerospace applications, consist of ceramic fibres embedded in a ceramic matrix, an interphase being usually introduced between the two constituents in order to control the fibre–matrix bonding. A convenient choice of these three components can lead to materials with outstanding thermomechanical properties even in an oxidizing environment [1].

The processing of these materials can be performed according to three classical ways, i.e. from the gaseous, liquid or solid phases [2–4]. The chemical vapour infiltration (CVI) technique, which derives directly from chemical vapour deposition (CVD), permits densification of the pore network of fibre preforms by a ceramic matrix, with several advantages: (i) a processing temperature rather low with respect to that of sintering, melting or decomposition of the ceramic matrix and (ii) a low processing pressure, both preventing a pronounced degradation of the ceramic fibres, and (iii) the possibility of preparing a large range of matrices and/or interphases [5–10]. Nevertheless, the isothermal/isobaric technique (I-CVI) exhibits two drawbacks: (i) a large processing duration resulting from the need for a low deposition rate to decrease the thickness gradient through the preform and (ii) a non-negligible residual porosity (about 10–15%).

With a view to solving these problems, derived methods have been proposed. Forced CVI, i.e. with temperature and/or pressure gradients, permits an increase of the infiltration rate but can only be applied to a very small number of specific samples such as tubes or plates [11]. The second technique is the pulse CVI (P-CVI) method developed by Beatty [12] and more recently by Sugiyama and co-workers [13, 14] for the infiltration of porous carbon or fibre preforms. In this process, a pressure cycle is applied in order to periodically regenerate the whole gas phase: the pulse consists, after evacuation of the reactor chamber, in instantaneous charging with source gas, holding at the desired pressure and again evacuation. The aim of this pressure cycling is to limit the occurrence of reaction products (usually inhibitory) within the preform pore network, and consequently to favour in-depth deposition and increase the infiltration rate.

The present paper is the first part of a study of the P-CVI of pyrocarbon. It deals mainly with the surface deposition process (P-CVD) of pyrocarbon through an investigation of the influence of various parameters such as the temperature, pressure, residence time and nature of gaseous precursor. This approach is carried out on model porous substrates which permit one to consider both the external surface and in-depth deposition.

0022–2461

2. Experimental procedure

2.1. P-CVD/CVI apparatus

The apparatus used for the CVD/CVI experiments is shown in Fig. 1. The precursor gas (here propane or methane) is maintained at the pressure desired for the pulse in a tank from which the gas can be fed to the reactor instantly through a pneumatic valve with an opening time of about 0.1 s. The deposition chamber is a vertical cylindrical Inconel tube resistively heated. The temperature is monitored with a thermocouple and a quasi-isothermal zone 27 mm in diameter and 50 mm in height is available. An outlet pneumatic valve permits evacuation of the gas mixture from the reactor chamber to the vacuum pump through a liquid nitrogen trap. An automatic device can control the opening and closing of the valves as well as the safety devices for temperature and pressure and also the total number of pulses. A typical example of a pressure cycle is given in Fig. 2.

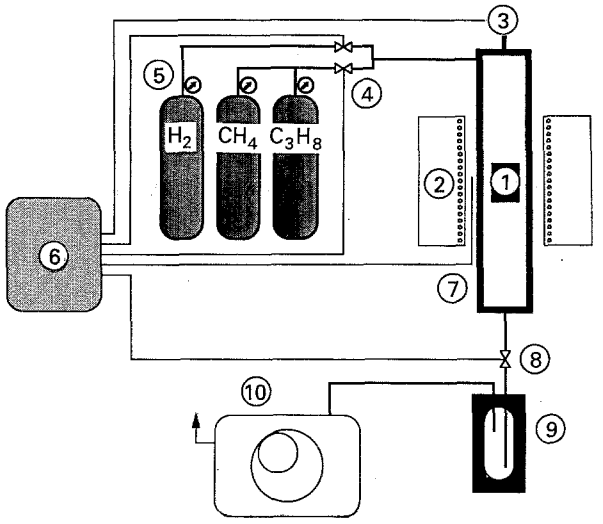

Figure 1 Apparatus used for the P-CVD/CVI of pyrocarbon (schematic): (1) substrate, (2) furnace, (3) pressure sensor, (4) gas injection valves, (5) gaseous sources, (6) automatic controller, (7) thermocouple, (8) shut-off valve, (9) liquid nitrogen trap, (10) vacuum pump.

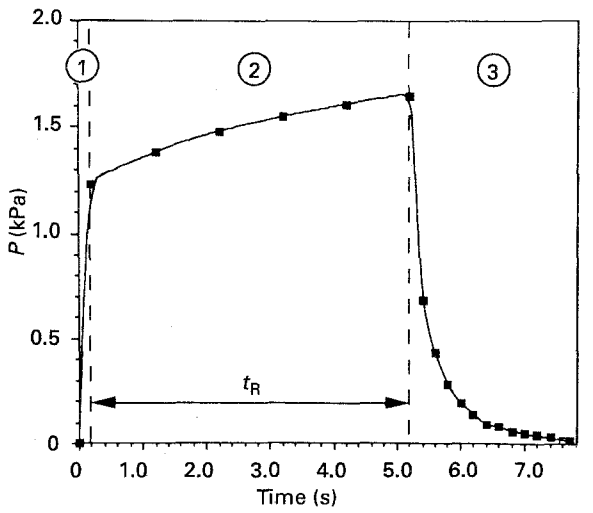

Figure 2 Example of pressure cycling for $t_R = 5$ s: (1) introduction (0.2 s), (2) deposition (5 s), (3) gas evacuation (2.5 s).

2.2. Model substrates

The model substrate with straight rectangular pores is shown schematically in Fig. 3. The model pores are formed by the assembly of two plates made of purified graphite, one of them being machined to obtain three parallel grooves. These grooves 20 mm in length exhibit rectangular cross-sections with the same width ($l = 2$ mm) and various heights ($h = 60$, 120 and 320 μm). The pore height is actually dependent on the tightening of both plates and the roughness of the graphite surface, which results in a possible uncertainty in h of about 5 μm. The practical interest of such a substrate is the easy assessment of the profiles of pyrocarbon deposit thickness by optical observations over the whole pore length, the deposits resulting from P-CVD being analysed on the external parts of the graphite plates.

2.3. Analysis of the gas phase

The chemical composition of the gaseous mixture was semi-quantitatively assessed by probing the gas phase near the substrate external surface with a capillary connected to a quadrupole mass spectrometer. The resulting analysis gave interesting data on the species stable at the ambient temperature, particularly on the variations of their concentration as a function of residence time (the Ar peak being used as a standard and the analysis duration being only 0.1 s).

2.4. Deposit analysis

The profiles of pyrocarbon deposit thickness were assessed by optical observations over the whole pore length, which necessitated cutting the sample axially, embedding it in a resin and performing conventional polishing. In the present work, the thickness of the deposits on the external surface of the substrates was more specifically investigated as a function of various experimental parameters.

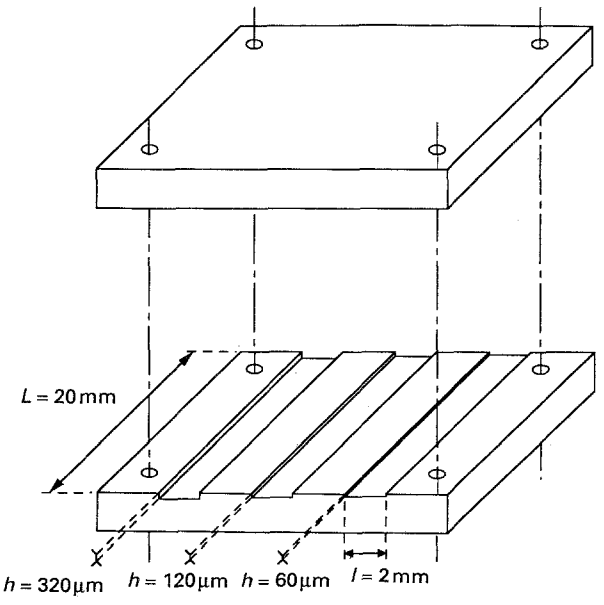

Figure 3 Schematic diagram of the model graphite substrate with three straight pores with rectangular cross-sections.

The surface morphology of the pyrocarbon was observed by scanning electron microscopy (SEM) either on the external deposits or on the in-depth deposits after separating the two plates of the model substrates. A preliminary microstructural approach was carried out by optical microscopy in polarized light.

3. Results

3.1. Analysis of the gas phase

In most of the experimental conditions, the main gaseous species detected by mass spectrometry are H_2, CH_4, C_2H_6, C_3H_8, C_2H_4, C_3H_6, C_2H_2 and C_6H_6. Several of these molecules exhibit mass spectra which overlap one another. Only the peaks for the masses 2, 16, 29 and 78 corresponding respectively to hydrogen, methane, propane and benzene are considered in the semi-quantitative analysis. On the other hand, tars are observed in the cold parts of the reactor and analysis by steric exclusion chromatography suggest that aromatic compounds such as pyrene and phenanthrene are formed.

The relative concentrations of H_2, CH_4, C_3H_8 and C_6H_6 are reported in Fig. 4 as a function of the residence time t_R for pure propane as precursor, $P = 3$ kPa and two values of the temperature, $T = 950$ and 1050 °C. While the C_3H_8 concentration decreases with increasing t_R, those of CH_4 and H_2 rise. These concentration variations are less and less rapid as t_R increases and a stable state seems to be reached beyond a threshold value of t_R. This threshold is about 30 s at 950 °C and only 15 s at 1050 °C. C_6H_6 is detected, but its concentration remains very low with respect to the other species.

The influence of temperature on the various species concentrations is shown in Fig. 5 for $t_R = 10$ s and two precursors: propane under 3 kPa and methane under 10 kPa. With increasing temperature, the C_3H_8 source species is more and more consumed, giving rise to increasing amounts of CH_4, H_2 and to a lesser extent C_6H_6. When CH_4 is the precursor species, its concentration is also decreased but no other species can be detected by the mass spectrometer.

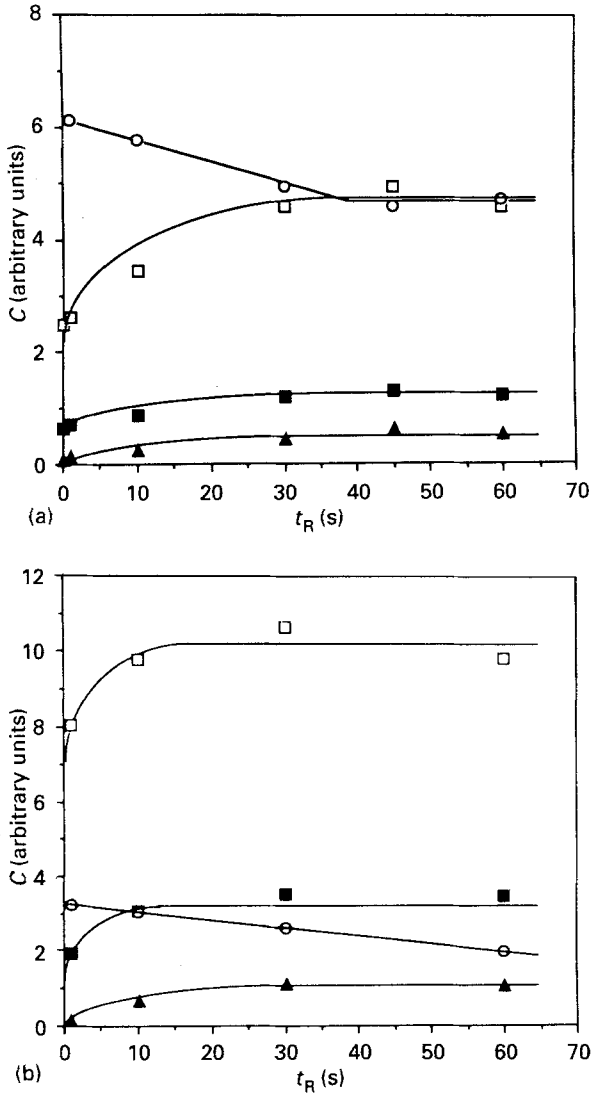

Figure 4 Variations of the concentrations of the various gaseous species analysed by mass spectrometry as a function of the residence time for $P = 3$ kPA: (a) $T = 950$ °C, (b) $T = 1050$ °C. (■) H_2, (□) CH_4, (○) C_3H_8, (▲) C_6H_6 (×20).

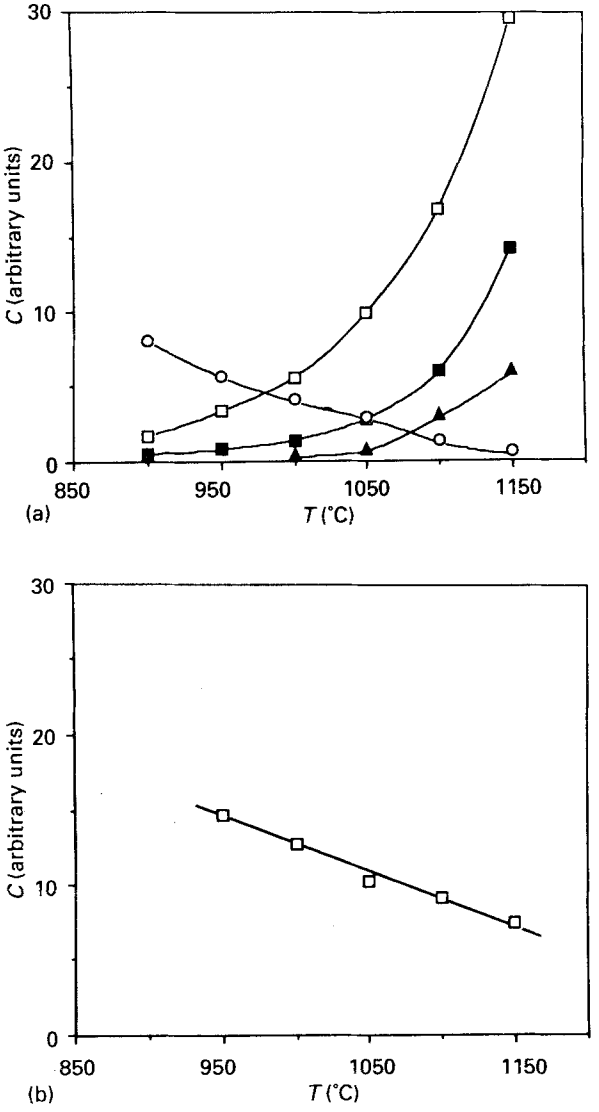

Figure 5 Variations of the concentrations of the various gaseous species analysed by mass spectrometry as a function of the temperature for $t_R = 10$ s: (a) $P(C_3H_8) = 3$ kPa, (b) $P(CH_4) = 10$ kPa. (■) H_2, (□) CH_4, (○) C_3H_8, (▲) C_6H_6 (×20).

3.2. Morphology of the deposits

The SEM micrograph of Fig. 6 shows the appearance of the pyrocarbon deposited at the entrance of a pore 320 μm in height for $T = 1050\,°C$, $P = 10\,kPa$ propane and $t_R = 2$ s. The deposit thickness seems to be rather uniform in cross-section, with a more or less smooth surface morphology. The pyrocarbon deposit consists of carbon layers almost parallel to the substrate surface and which appear only weakly bonded to one another.

As shown in Fig. 7, the pyrocarbon has grown with a cone-columnar microstructure [15]. Most of the nucleation sites are located on the rough graphite substrate surface for various experimental conditions, e.g. for $P = 3\,kPa$, $T = 1050\,°C$ and $t_R = 0.5$ s (Fig. 7a). If the propane pressure is high enough ($P \geqslant 10\,kPa$) the nucleation frequency is much higher, giving rise to a lot of small growth cones within the pyrocarbon deposit (Fig. 7b).

3.3. Kinetics of the pulsed deposition of pyrocarbon

3.3.1. Influence of residence time

Fig. 8 shows the variations of the thickness of pyrocarbon deposited during one pulse (overall thickness divided by the pulse number) on the external surface (e_{ps}) and at the centre of pores of height 320 μm (e_{p320}) and 60 μm (e_{p60}), as a function of the residence time t_R for a temperature of 1050 °C and three values of the propane pressure ($P = 1$, 3, and 10 kPa). All the observed thicknesses seem to increase in a parabolic manner with t_R up to a threshold value (beyond which they are almost constant). This parabolic law is evidenced in the case of surface deposition by drawing the variations in a double logarithmic scale (Fig. 9):

$$e_{ps} = At_R^{0.5} \quad (1)$$

where A is a constant which depends on the pressure and temperature deposition conditions. This behaviour means that, during a long enough pulse, the instantaneous deposition rate decreases continuously down to zero.

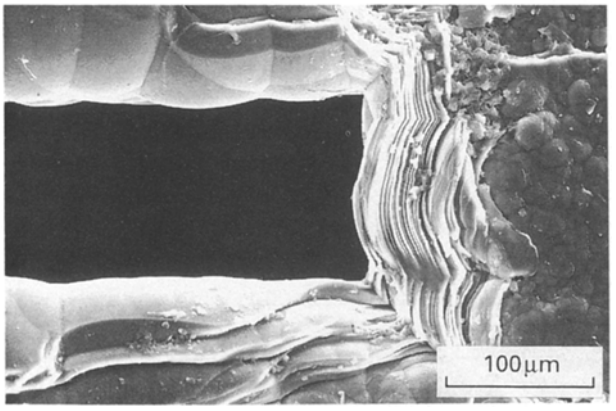

Figure 6 SEM micrograph of pyrocarbon deposited at the entrance of a 320 μm model pore for $T = 1050\,°C$, $P(C_3H_8) = 10\,kPa$ and $t_R = 2$ s.

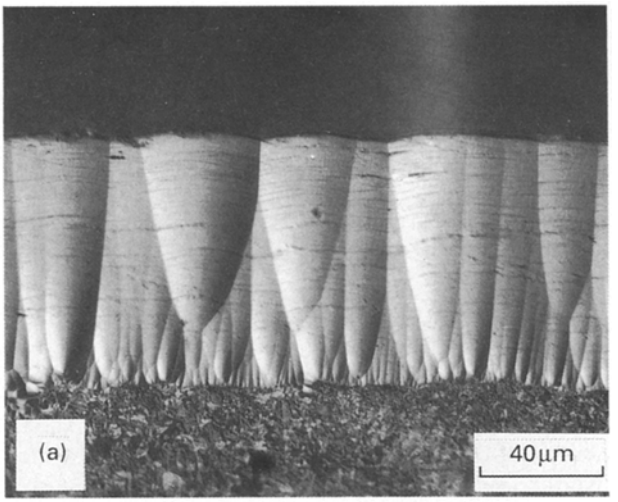

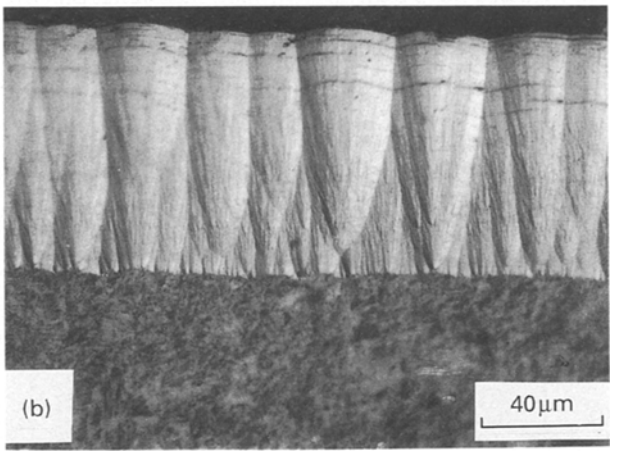

Figure 7 Optical micrographs (polarized light) of pyrocarbon deposited from propane for $T = 1050\,°C$ and (a) $P = 3\,kPa$, $t_R = 0.5$ s and (b) $P = 10\,kPa$, $t_R = 2$ s.

3.3.2. Influence of temperature

Fig. 10 shows the thermal variations of the deposit thicknesses (e_{ps}, e_{p320}, e_{p120} and e_{p60}) (Arrhenius plots) for three typical residence time values. For a short time ($t_R = 0.5$ s), i.e. when the instantaneous deposition rate is relatively high, the thickness of pyrocarbon deposited per pulse on the external surface of the substrate is highly favoured by raising the temperature. For a long residence time ($t_R = 60$ s), at the end of which the growth rate is zero, the thickness of pyrocarbon deposited after one pulse increases more slowly with temperature. For an intermediate time ($t_R = 10$ s), two regimes are observed for both the surface and in-depth depositions: a high dependence at low temperatures and a low dependence at high temperatures, with a transition at about 1025 °C. For the smallest pore ($h = 60$ μm), the deposition at its centre is not favoured by increasing the temperature.

3.3.3. Influence of pressure

The variations with pressure of the pyrocarbon thickness deposited per pulse at the external surface (e_{ps}) are shown in Fig. 11 in a double logarithmic scale for

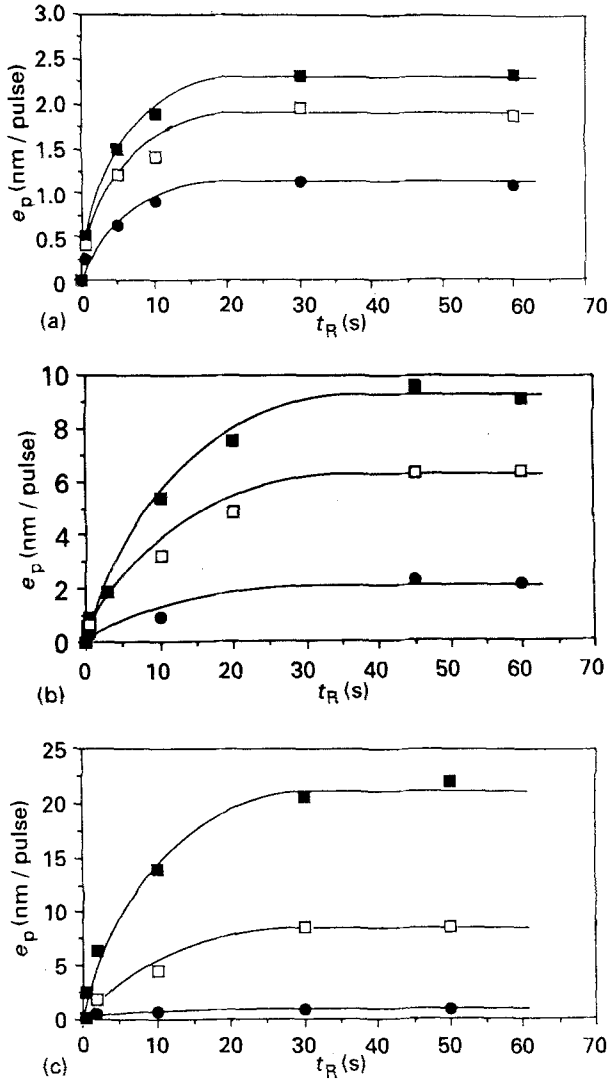

Figure 8 Variations with residence time of deposit thickness per pulse (■) on the external surface, (□) at the centre of a pore of height 320 μm and (●) at the centre of a pore of height 60 μm. Propane pressure (a) 1 kPa, (b) 3 kPa, (c) 10 kPa; temperature 1050 °C.

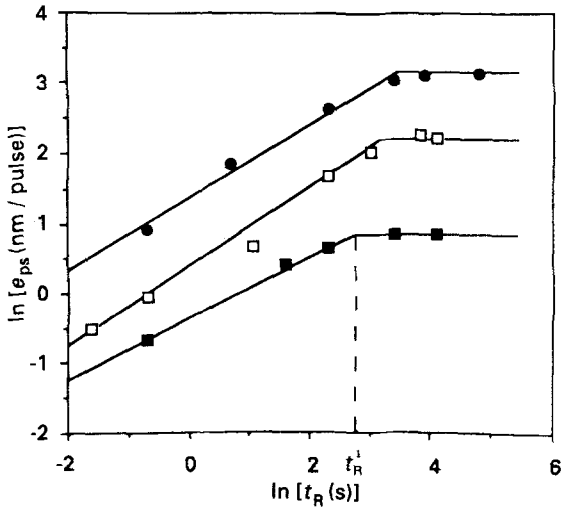

Figure 9 Variations of deposit thickness per pulse on the external surface of the substrate as a function of the residence time (double logarithmic plot) for various total propane pressures and $T = 1050\,°C$: (■) 1 kPa, $\ln e_{ps} = -0.35 + 0.45 \ln t_R$; (□) 3 kPa, $\ln e_{ps} = 0.30 + 0.55 \ln t_R$; (●) 10 kPa, $\ln e_{ps} = 1.37 + 0.51 \ln t_R$.

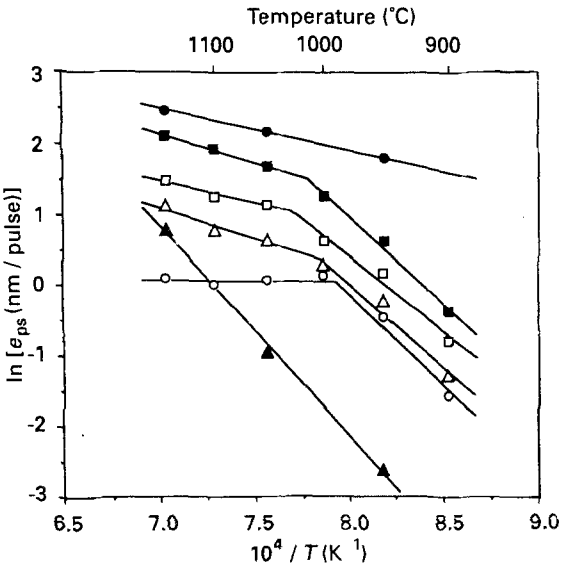

Figure 10 Variations with reciprocal temperature of deposit thickness per pulse on the external surface of the substrate for residence time (▲) 0.5 s, (■) 10 s and (●) 60 s, and at the centre of pores of height (○) 60 μm, (△) 120 μm and (□) 320 μm for $t_R = 10$ s; $P(C_3H_8) = 3$ kPa.

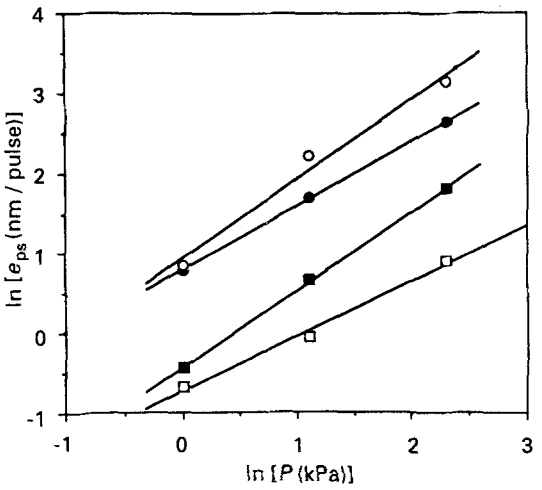

Figure 11 Variations of deposit thickness per pulse on the external substrate surface as a function of propane pressure for various residence times and temperatures: (■) $T = 950\,°C$, $t_R = 10$ s, $\ln e_{ps} = -0.44 + 0.97 \ln P$; (□) $T = 1050\,°C$, $t_R = 0.5$ s, $\ln e_{ps} = -0.72 + 0.69 \ln P$; (●) $T = 1050\,°C$, $t_R = 10$ s, $\ln e_{ps} = 0.79 + 0.80 \ln P$; (○) $T = 1050\,°C$, $t_R > t_R^1$, $\ln e_{ps} = 0.94 + 0.99 \ln P$.

$T = 1050\,°C$ and the three values of t_R previously given and for $T = 950\,°C$ and $t_R = 10$ s. For all the conditions, a linear variation is observed with a slope between 0.7 and 1, which can be expressed by the following law:

$$e_{ps} = B P^n \qquad (2)$$

with $0.7 \leqslant n \leqslant 1$ and B a constant which depends on the temperature and residence time.

3.3.4. Influence of pore size

The deposit thickness per pulse at the centre of the pores is reported as a function of the pore height h in Fig. 12 for various conditions of propane pressure,

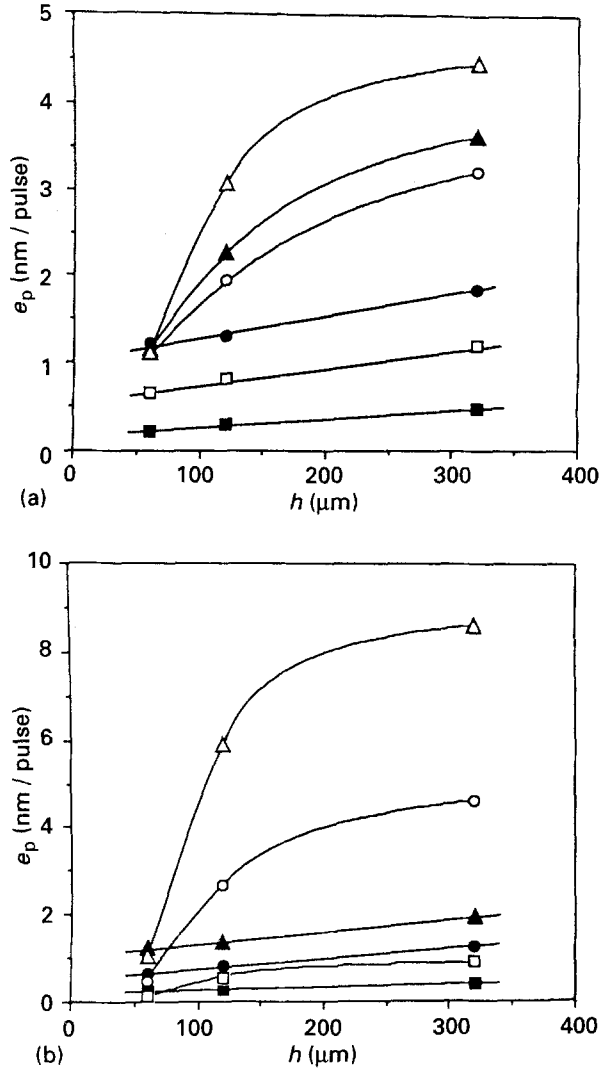

Figure 12 Variations of the deposit thickness per pulse from propane at the centre of the pores as a function of their height. (a) $P = 3$ kPa, $t_R = 10$ s and temperature (■) 900 °C, (□) 950 °C, (●) 1000 °C, (○) 1050 °C, (▲) 1100 °C, (△) 1150 °C. (b) $T = 1050$ °C and (■) $P = 1$ kPa, $t_R = 0.5$ s; (□) 10 kPa, 0.5 s; (●) 1 kPa, 5 s; (○) 10 kPa, 5 s; (▲) 1 kPa, 60 s; (△) 10 kPa, 60 s.

temperature and residence time. If the thickness is found to increase with pore height in all cases, two different behaviours are observed: (i) for low temperatures ($T \leqslant 1050$ °C) and low pressures ($P \leqslant 3$ kPa) a linear variation occurs, while (ii) for high temperatures ($T \geqslant 1050$ °C) and high pressures ($P \geqslant 3$ kPa) the small pores ($h = 60$ μm) are hardly infiltrated, giving rise to a non-linear variation. An increase of the residence time increases the deposit thickness per pulse but does not affect the type of variation.

3.3.5. Influence of the precursor

Table I gives a comparison of the various pyrocarbon thicknesses, e_{ps}, e_{p320} and e_{p60}, for propane and methane as source species, $P = 1$, 3 and 10 kPa, $T = 1050$ °C and $t_R = 10$ s. The external deposit thickness e_{ps} is highly decreased (by a factor of about 10) if CH_4 replaces C_3H_8 as precursor. On the other hand, CH_4 as precursor permits a much better infiltration, the thicknesses per pulse at the centre of the pores being close to those measured at the external surface.

TABLE I Thickness of pyrocarbon deposited per pulse at the external substrate surface and at the centre of 320 and 60 μm pores for $T = 1050$ °C, $t_R = 10$ s, $P = 3$ or 10 kPa, and propane and methane as precursors

P (kPa)	Gas	e_{ps} (μm)	e_{p320} (μm)	e_{p60} (μm)
3	Propane	5.4	3.2	0.97
	Methane	0.4	0.46	0.30
10	Propane	14.0	4.5	0.46
	Methane	1.4	0.97	0.42

For $P = 3$ kPa and a pore of 320 μm height, the in-depth deposit thickness is slightly higher than the surface one.

4. Discussion

In P-CVD/CVI the chemical system is maintained at a constant pressure during the residence time, without any exchange with the outside, the reactor being a closed system. In such a case, the gaseous phase introduced in the reactor is changed according to a series of reactions which are well known for methane: cracking, cycling and aromatization, as shown by Kassel [16], Grisdale [17] or Chen and Back [18]. This "maturation" of the gas phase, which probably controls the deposition process of pyrocarbon, depends on the various parameters previously studied, i.e. t_R, T, P, precursor nature and pore size for P-CVI.

4.1. Influence of t_R, T and P

The variations of pyrocarbon thicknesses per pulse with residence time represented in Fig. 8 are very similar to those reported by Sugiyama and Ohzawa [14] for P-CVD/CVI of boron nitride on an Si_3N_4-based preform. They have also been correlated with the variations of species concentrations (Fig. 4). A parabolic increase of both the concentrations of species produced (H_2, CH_4, C_6H_6) and deposit thicknesses per pulse is observed as a function of t_R up to a threshold value t_R^1. Beyond t_R^1, no more reaction seems to occur. Nevertheless, thermodynamic equilibrium is not achieved because if it was reached under the presently studied conditions, CH_4 should be hardly detected by gas phase analysis, being almost totally consumed to give pyrocarbon [19]. Kinetic factors such as an inhibition effect by hydrogen can limit the deposition reactions which lead to the thermodynamic equilibrium. For $t_R = t_R^1$, the gas phase maturation can be considered as finished. When the temperature increases, this maturation is more and more rapid and t_R^1 decreases. t_R^1 increases slowly with the precursor pressure corresponding to a higher amount of precursor species to be consumed which is, in part, compensated by the increase of the source consumption rate.

4.2. Influence of pore size

The occurrence of two kinds of behaviour in terms of infiltration quality (see section 3.3.4 and Fig. 12) suggests that different mechanisms with modification of

the reaction intermediates are involved in the P-CVD/CVI process. Under conditions of high pressures and high temperatures, the small pores are difficult to infiltrate whatever the residence time (Fig. 12). This result means that a high extent of gas phase maturation is rapidly reached, giving rise to large aromatic molecules. The diffusion of such intermediate species towards the centre of the small pores is very difficult. They are instead stuck on the external surface of the substrate or at the entrance of the pores according to a process previously described [20]. Conversely, for low pressures and low temperatures, the extent of gas phase maturation is very limited with the occurrence of only small-sized molecules. These species easily diffuse along the pores (even the small ones), which results in few differences between the infiltration qualities of pores with various sizes.

4.3. Influence of the precursor

Owing to its higher thermal stability, the cracking of CH_4 is slower than that of C_3H_8, giving rise to a lower extent of gas phase maturation for a given residence time. Consequently, (i) the thickness of the external deposits for one pulse is lower in the case of methane and (ii) the infiltration process is better, resulting from the easier diffusion of the small source species occurring in a not very matured gas phase (Table I). In addition, a reverse infiltration gradient can be obtained for specific conditions such as $T = 1050\,°C$, $P = 3\,kPa$ and a $320\,\mu m$ pore. This singular result could be explained on the basis of a progressive maturation of the gas phase during mass transport along the pores, the deposition from heavy aromatic species being more rapid than the deposition from light species.

5. Conclusions

The process of the P-CVD/CVI of carbon from propane can be described as successive identical cycles, each one including three main steps: (i) inflow of the gaseous precursor by forced convection within the reactor and the pores of the substrate; (ii) holding of the gaseous phase at a given pressure which results partly in the deposition of pyrocarbon from small molecules, the production of mainly hydrogen and CH_4 and the diffusion of reactants and products through concentration gradients, partly in maturation of the gas phase with the formation of heavier and more dehydrogenated aromatic species that are easily be stuck to the substrate surface; and (iii) removal of the gaseous mixture from the pores of the substrate and the reactor by forced convection.

On the basis of the present study, at least two types of mechanism, governed by maturation of the gas phase, have been evidenced: (i) mechanism I for low pressures, low temperatures and stable precursors such as CH_4, where gas maturation is very limited and deposition mainly occurs by slow decomposition of small molecules resulting in a lateral growth of PyC; and (ii) mechanism II for high pressures, high temperatures and more reactive precursors such as C_3H_8, where a high maturation of the gas phase results in rapid condensation of heavy aromatic species stacking on the substrate surface.

Actually, according to experimental conditions (T, P, t_R) only the first mechanism or both occur during a pulse and the contribution of one of these mechanisms is probably highly dominant.

The two possible mechanisms derived from the present study of the P-CVD/CVI process result in different microstructures of pyrocarbon and different infiltration qualities. Such correlations will be the aim of the companion article (Part 2 [21]).

Acknowledgements

This work has been supported by SEP. The authors are indebted to C. Robin-Brosse from SEP for valuable discussions.

References

1. R. NASLAIN, "Introduction aux materiaux composites 2–Matrices métalliques et céramiques" (CNRS/IMC, Bordeaux, 1985).
2. R. NASLAIN and F. LANGLAIS, in "High Temperature Science", Vol. 27, edited by J. W. Hastie (Humana, Clifton, New Jersey 1990) p. 221.
3. S. YAJIMA, *Ceram. Bull.* **62**, (1983) 893.
4. J. K. GUO, Z. Q. MAO, C. D. BAO, R. H. WANG and D. S. YAN, *J. Mater. Sci.* **117** (1982) 3611.
5. F. CHRISTIN, R. NASLAIN and C. BERNARD, in Proceedings of 7th International Conference on CVD, edited by T. O. Sedgwick and H. Lyoltin (Electrochemical Society, Princeton, 1979) p. 499.
6. J. Y. ROSSIGNOL, F. LANGLAIS, R. NASLAIN and C. BERNARD, in Proceedings of 9th International Conference on CVD, edited by M. D. Robinson C.H.J. van den Brehel, G. W. Culler, J. M. Bloccher, Jr., and P. Ray-Choudhury (Electrochemical Society, Pennington, 1984) p. 596.
7. H. HANNACHE, F. LANGLAIS and R. NASLAIN, in Proceedings of 5th European Conference on CVD, Uppsala, 1985, edited by J. O. Carlsson and J. Lindström, p. 219.
8. H. HANNACHE, R. NASLAIN and C. BERNARD, *J. Less-Common Met.* **95** (1983) 221.
9. R. COLMET, R. NASLAIN, P. HAGENMULLER and C. BERNARD, in Proceedings of 8th International Conference on CVD, edited by J. M. Blocher Jr., G. E. Whillard and G. Wahl (Electrochemical Society, Pennington, 1981) p. 17.
10. J. MINET, F. LANGLAIS and R. NASLAIN, *J. Less-Common Met.* **132** (1987) 273.
11. T. M. BESMANN, R. A. LOWDEN, D. P. STINTON and L. L. STARR, in Proceedings of 7th European Conference on CVD, *J. Physique*, Colloque C5, Suppl. 5, **50** (1989) 229.
12. R. L. BEATTY, *J. Nucl. Appl. Technol.* **8** (1970) 488.
13. K. SUGIYAMA and T. NAKAMURA, *J. Mater. Sci. Lett.* **6** (1987) 331.
14. K. SUGIYAMA and Y. OHZAWA, *J. Mater. Sci.* **25** (1990) 4511.
15. L. F. COFFIN, *J. Amer. Ceram. Soc.* **47** (1964) 473.
16. L. S. KASSEL, *ibid.* **54** (1932) 3949.
17. R. O. GRISDALE, *J. Appl. Phys.* **24** (1953) 1082.
18. C. J. CHEN and M. H. BACK, *Carbon* **17** (1979) 175.
19. H. MELLOTTÉE, Thèse de l'Université de Paris (1968).
20. J. L. KAAE, *Carbon*, **23** (1985) 665.
21. P. DUPEL, R. PAILLER, X. BOURRAT and R. NASLAIN, *J. Mater. Sci.* **28** (1993) JM30372.

Received 25 June
and accepted 24 August 1993